Molecular Crystals and Liquid Crystals Science and Technology. Section A. Molecular Crystals and Liquid Crystals

Publication details, including instructions for authors and subscription information:
http://www.tandfonline.com/loi/gmcl19

Phase Separation Dynamics in a Mixture of Polystyrene and Liquid Crystal

W.-K. Kim [a] & T. Kyu [a]

[a] Institute of Polymer Engineering, The University of Akron, Akron, OH, 44325

Version of record first published: 24 Sep 2006.

To cite this article: W.-K. Kim & T. Kyu (1994): Phase Separation Dynamics in a Mixture of Polystyrene and Liquid Crystal, Molecular Crystals and Liquid Crystals Science and Technology. Section A. Molecular Crystals and Liquid Crystals, 250:1, 131-141

To link to this article: http://dx.doi.org/10.1080/10587259408028199

Mol. Cryst. Liq. Cryst., 1994, Vol. 250, pp. 131–141
Reprints available directly from the publisher
Photocopying permitted by license only

Printed in the United States of America

Phase Separation Dynamics in a Mixture of Polystyrene and Liquid Crystal

W.-K. KIM and T. KYU*

Institute of Polymer Engineering, The University of Akron, Akron, OH 44325

(Received June 2, 1993; in final form September 15, 1993)

A phase diagram for a mixture of polystyrene (PS) and monomeric liquid crystal (E7) was established on the basis of differential scanning calorimetry and cloud point measurements. An upper critical solution temperature (UCST) type phase diagram, overlapping with a nematic-isotropic transition of liquid crystals, was observed. Several deep temperature quenches were undertaken at an off-critical compositon (60/40 PS/E7) from a single phase to a two-phase region. Time-evolution of the structure factor was determined by time-resolved static light scattering. Phase separation appeared to occur via spinodal decomposition (SD) with a growth exponent of 1/3 at deep quenches in conformity with the cluster dynamic theory. A nucleation and growth (NG) was discerned at a shallower temperature quench.

Keywords: Phase separation, spinodal decomposition, nematic-isotropic transition, polymer dispersed liquid crystal, UCST.

INTRODUCTION

In recent years, the emergence of liquid crystal display technology has provoked the interest of academia and industries.[1] Polymer dispersed liquid crystal (PDLC) films are optical devices which have potential for applications such as optical switches and variable transmittance windows.[1,2] The PDLC device operates by electrically controlling the refractive index of a liquid crystal (LC) to match that of an optically transparent polymer matrix. The LC molecules are usually confined to micron-sized droplets dispersed in the matrix. In the absence of a field, the LC directors in the droplets are randomly aligned. This leads to a mismatch of LC and matrix refractive indices, giving rise to light scattering and opaque appearance. When the PDLC film is subjected to an external electric field across the film thickness, the directors orient parallel to the field (film normal) direction. In this oriented state, the film is transparent to naked eye since the ordinary refractive index of the LC can be matched approximately with the index of the matrix. When the electric field is switched off, the film reverts to its turbid state.

PDLC films are commonly prepared by phase separating an initially homogeneous mixture of monomeric liquid crystal/polymer either by thermal quenching,[3,4] chemical or photochemical cross-linking of matrix polymers or by solvent evaporation.[1,2]

* To whom correspondence should be addressed.

During thermal quenching, the nematic LC crystals segregate out and form droplets or an interconnected network structure depending on the mechanisms of phase separation and kinetics of phase growth. This aspect of domain formation has not been studied systematically, although the effect of the shape, the size and the dispersion of these LC domains on the electro-optical performance has been recognized for some time.[5] The understanding of thermodynamics and kinetics of phase decomposition in PDLCs is therefore crucial to gain control of the domain structure of PDLC films, and ultimately their electro-optical properties.[5]

In this paper, we first establish a phase diagram for a narrow molecular weight PS/E7 systems by using a cloud point method. We used optical microscopy and light scattering to monitor the time-evolution of the structure factor. The kinetic results were analyzed in the framework of non-linear and dynamic scaling theories.

EXPERIMENTAL

Materials

A main chain liquid crystal, commercially known as E7, was purchased from EM Industries (manufactured by BDH) and used as the dispersing phase. E7 is a mixture of cyanobiphenyl (CB) moieties, comprising 5CB (51 wt%), 7CB (25%), oxy-cyanobiphenyl 8OCB (16%) and cyanotriphenyl 5CT (8%). Note that the prefix refers to the numbers of methylene linkages. Although the structure of E7 is seemingly complex, it displays a phase transition behavior reminiscent of that of a single-component nematic liquid crystal. That is to say, it exhibits a singel crystal-nematic transition at $-10°C$ and a single nematic–isotopic (N–I) transition at 61°C.[1,5] Thus, the E7 based PDLCs may be viewed as a pseudo two-phase system. Polystyrene (PS) used in this study was a narrow molecular weight fraction ($M_w = 218,000$; $M_w/M_n = 1.05$) from the Scientific Polymer Product, Inc.

PS was dissolved in tetrahydrofuran (THF) at ambient temperature by stirring rigorously using a magnetic stirrer. The polymer concentration was 3 wt%. E7 were added in desired amounts to make the blends. Film specimens were prepared on glass slides by evaporating THF. These films were cloudy in appearance, but became transparent upon heating above the N–I transition temperature of E7 and returned to a two-phase system upon cooling to ambient temperature.

Methods

The time-resolved light scattering set-up used in this study consists a Reticon one dimensional detector, Optical Multichannel Analyzer (OMA III, EG and G) and a sample hot stage controlled by a programmable temperature (Omega CN-2012). The Reticon detector has a resolution of 1024 pixels per 25 mm and one scan takes about 30 ms. The post data treatment was carried out on an off-line IBM PC-2/30. A 2 mW He-Ne laser with a wavelength of 632.8 nm was used as a light source.

DSC thermograms were acquired on a DuPont thermal analyzer (Model 9900) with a heating module (Model 910) under dry nitrogen circulation. The heating rate was

10°C/min unless otherwise specified. Optical micrographs were taken by a 35 mm Nikon camera attached to an optical microscope (Optiphot2-pol, Nikon).

RESULTS AND DISCUSSION

Cloud point temperatures were determined by measuring the abrupt change of scattered light at a given scattering angle ($\sim 10°$) during the course of cooling (Figure 1). It should be pointed out that the difference of cloud point temperatures in the cooling and heating cycles is within 1°C. At a liquid crystal/polymer concentration (e.g., 10/90 PS/E7), a two-step increase of intensity can be discerned (Figure 2). As will be discussed latter, the first increase of intensity may be associated with the phase separation between isotropic LC phase and polymer, whereas the second step may be attributed to a nematic LC formation within preformed LC droplets. The cloud point temperatures are plotted against E7 content in Figure 3. The nematic–isotropic (N–I) transition of the E7 at 61°C was also included in the plot. The phase diagram is basically that for a system exhibiting upper critical solution temperature (UCST) behavior. However, a nematic region exists at very high LC concentrations in excess of 90 wt%. There appears a narrow co-existence region consisting of the isotropic liquid and nematic phases as indicated in the phase diagram. The existence of such a narrow region has been predicted theoretically[6,7] in which the orientational order parameter was taken into account in the equation of the free energy of mixing. Such a complex phase diagram was determined experimentally by cloud point measurements.[4,8]

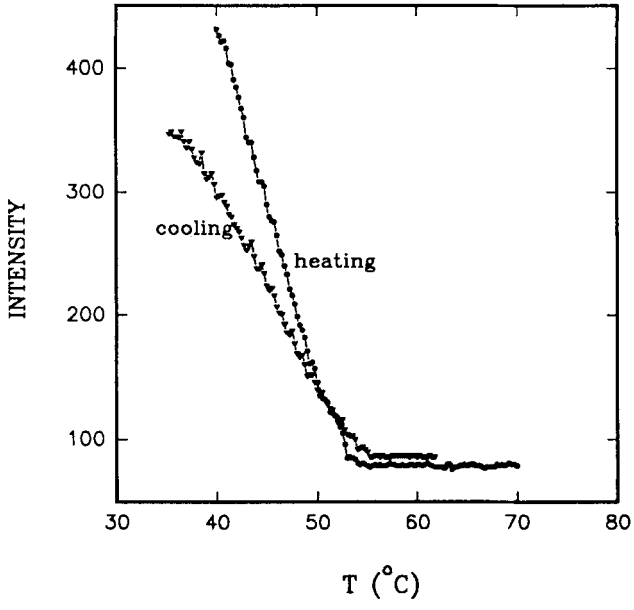

FIGURE 1 The variation of scattered light intensity at a given scattering angle during the course of heating and cooling. The rate was 0.25°C/min.

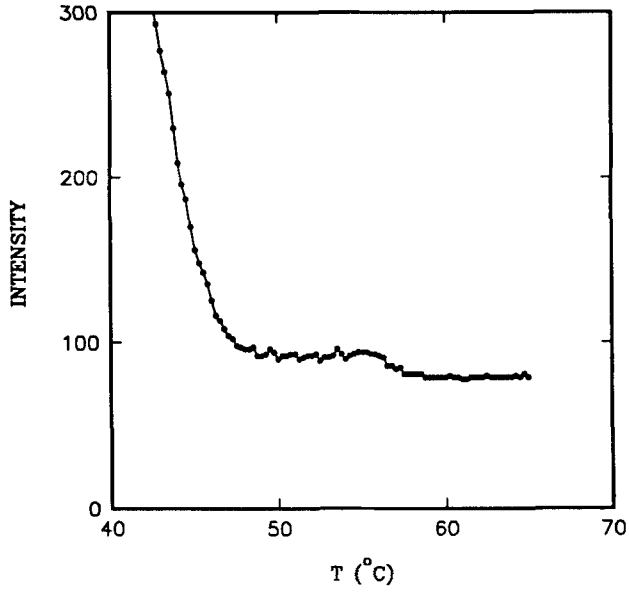

FIGURE 2 The change of scattered intensity at the 90% E7 composition during cooling at 0.25°C/min.

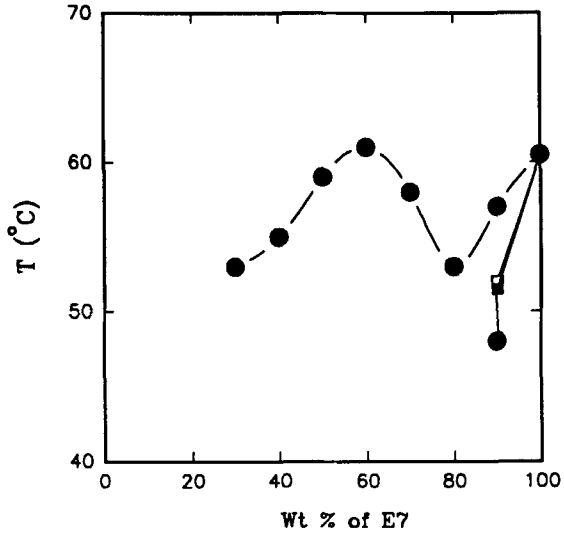

FIGURE 3 Phase diagram of the PS/E7 system based on cloud point, DSC and depolarized light scattering determinations. The closed circle represents cloud points while closed and open squares are from depolarized light scattering and DSC, respectively.

Recently, UCST behavior overlapping with nematic–isotropic transitions has been observed by DSC for uncured LC/matrix systems.[9]

The existence of nematic LC phase in the high E7 content compositions may be identified by DSC in Figure 4. In both heating and cooling cycles, the N–I transitions

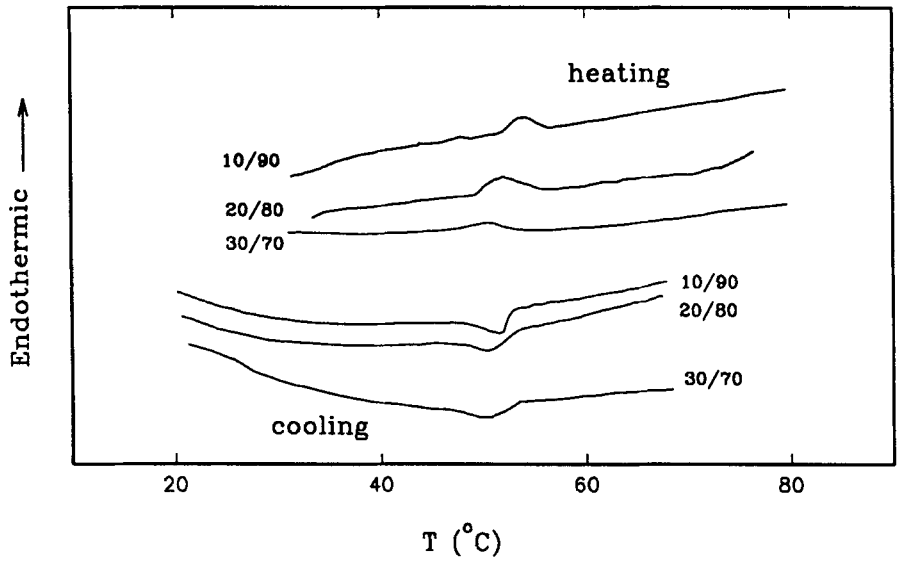

FIGURE 4 DSC endotherms of high E7 content compositions displaying nematic–isotropic transitions. The heating rate was 10°C/min.

can be observed. These transition temperatures can be confirmed further by depolarized Hv (horizontal polarizer with vertical analyzer) scattering because the Hv scattering is sensitive only to the orientation fluctuation arising from ordered structures. During the course of continuous cooling, the LC/polymer mixtures phase separate into LC-rich and LC-poor regions. The DSC scans often showed dual endotherms particularly in the intermediate compositions which may be affected by the extent of phase separation and its kinetics. Thus only the result of the 90 wt% E7 is incorporated in the phase diagram (Figure 3) as it is close to the co-existence line.

We also carried out several temperature quench experiments by rapidly transferring the PDLC films from a single phase temperature (100°C) to a two-phase region. A 60/40 PS/E7 composition was chosen because the N–I transition of the LC phase was not pronounced and considerably slow as compared with the liquid–liquid phase separation. This permits one to mimic the liquid–liquid phase separation process in a rigid molecule/coil polymer system. Figure 5 depicts the optical micrographs obtained as a function of elapsed time after a T quench to 25°C. Tiny interconnected structures develop and grow in time. The corresponding light scattering pictures (Figure 6) show that the diameter of the diffuse scattering halo shrinks while the intensity greatly increases with time, indicating an increase in length scale, i.e., phase growth. These structures are characteristic of spinodal decomposition (SD), although existence of such structures does not prove that SD is occurring.[9] By polarized optical microscopy, we observed no identifiable structure within the time scale of Figure 5. However, after several hours, some birefringent entities due to nematic formation could be discerned for the 60/40 PS/E7 composition; the structure is too vague to be seen clearly under the crossed polarizers. In the case of polymethyl methacrylate (PMMA)/E7 (60/40), distinct but complex structures, comprising of large phase separated domains and nematic

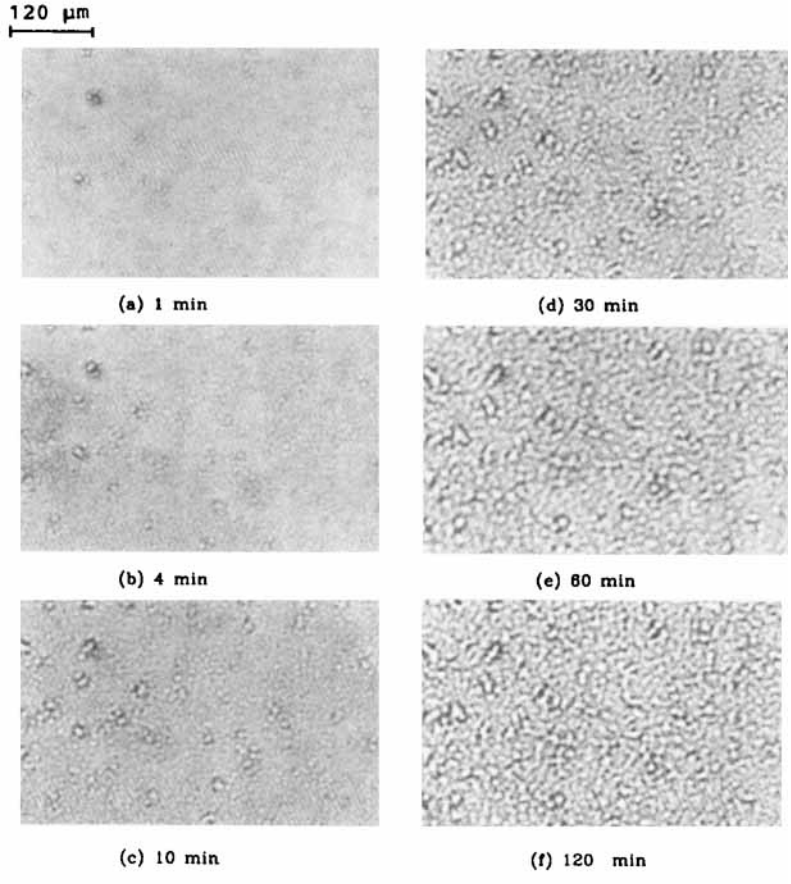

FIGURE 5 Time-evolution of phase separated domains for a 60/40 PS/E7 mixture following a T quench from 100°C to 25°C from optical microscopy.

disclinations, can be seen within a few minutes of phase separation.[8] This discrepancy in behavior may be attributed to the differences in the N–I transition temperatures of the two systems; T_{NI} for 60/40 PS/E7 is significantly (about 10°C) lower than that for 60/40 PMMA/E7. Another factor which could affect the nematic transitions is the difference in molecular weight, i.e., Mw of 218,000 for PS vs. 23,000 for PMMA. Hence, it is possible that nematic formation could be slowed down in the PS/E7 system relative to the PMMA/E7.

The growth dynamics of the length scale was studied following T quenches at the 60/40 PS/E7 composition by using time-resolved light scattering. For a shallow temperature quench to 52°C, the scattered intensity increases in time at all scattering angles without revealing a maximum (Figure 7). The lack of a scattering peak may be a consequence of nucleation and growth (NG) which generally occurs via a heterogeneous process which results in a distribution of droplet sizes. That is to say, the interparticle interference peaks may be washed out due to polydisperse domains,

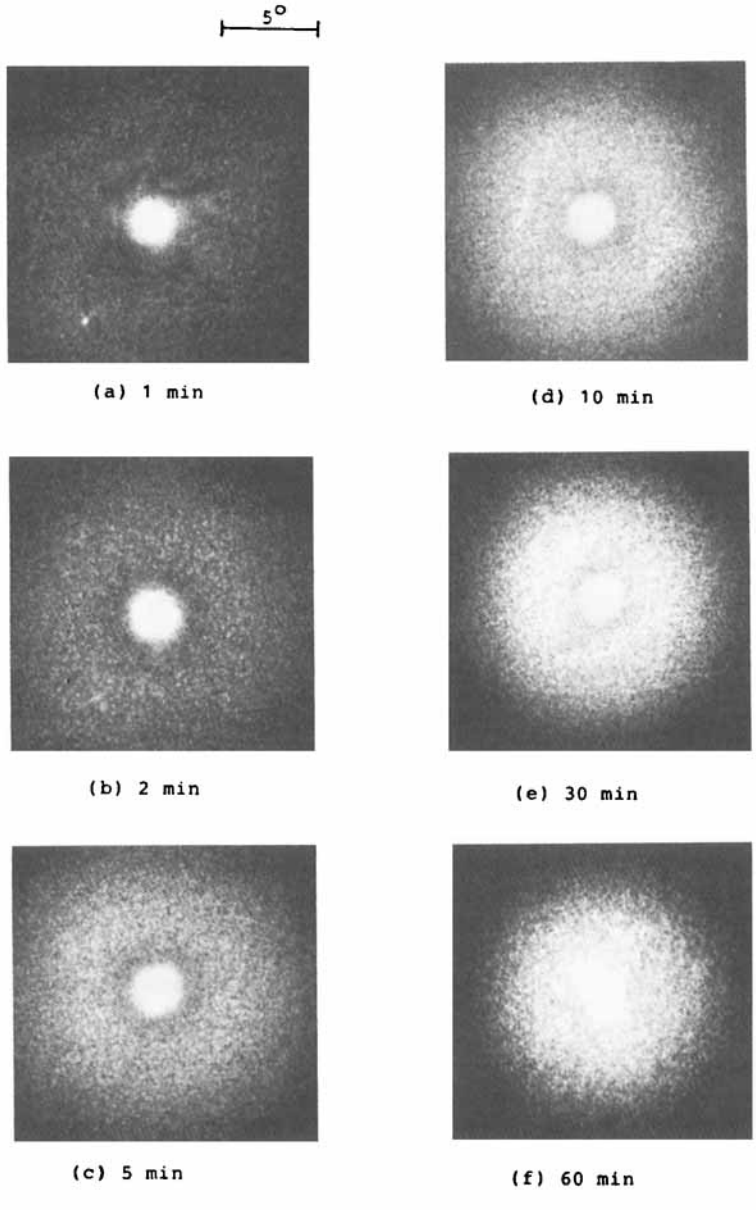

FIGURE 6 The change of unpolarized light scattering patterns with elapsed time for a 60/40 PS/E7 mixture following a T quench from 100°C to 25°C.

causing the scattered intensity to decay monotonically with increasing scattering angle. Recently, Cumming *et al.*[10] demonstrated that monodisperse droplets can be produced by the NG process in mixtures of polyisoprene and polyethylene–propylene with narrow distribution of low molecular weights. Light scattering from such monodisperse domains exhibits higher order scattering maxima in the structure factor, but

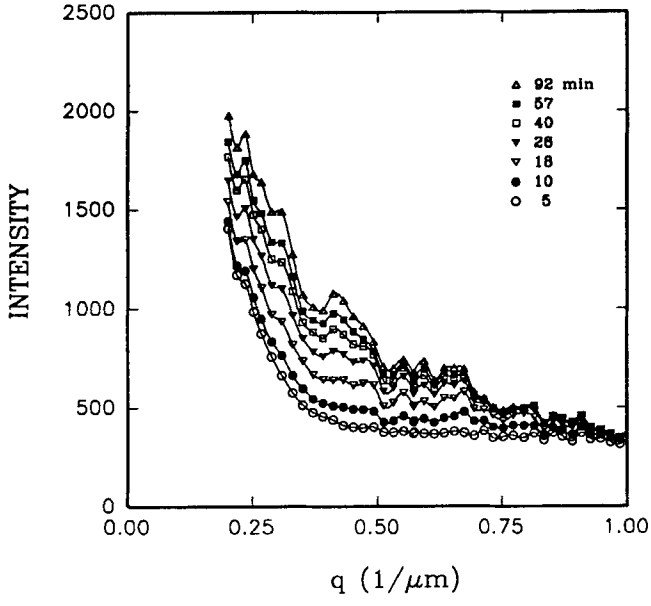

FIGURE 7 Time-evolution of structure factor following a T quench from a single phase (100°C) to a metastable region (52°C) for a 60/40 PS/E7 mixture.

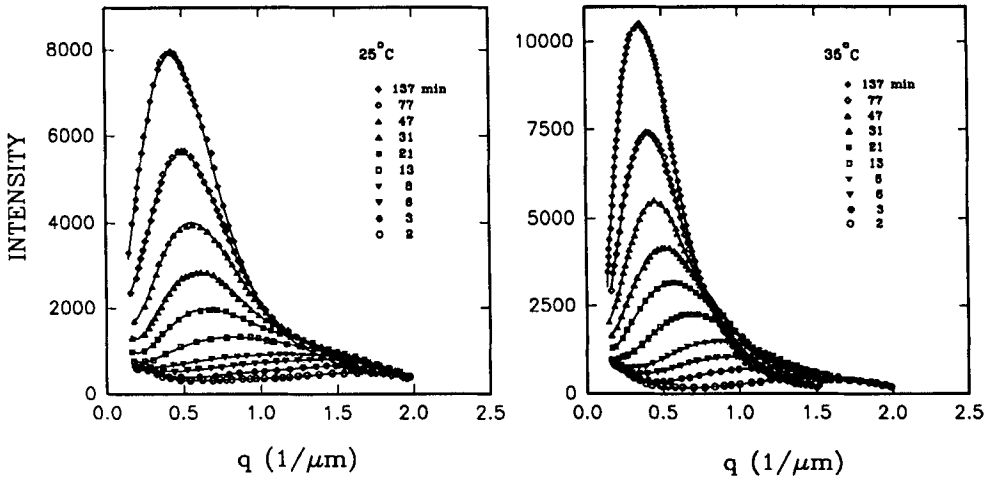

FIGURE 8 Time-evolution of structure factor following a T quench from 100°C to an unstable region for a 60/40 PS/E7 mixture (a) 25°C and (b) 35°C.

these multiple peaks disappear by merely increasing the polydispersity factor by about 7%.

On the other hand, for deep T quenches into an unstable region, a diffuse scattering peak can be observed. Figures 8(a,b) show the typical time-evolution of scattering profiles following T quenches from 100°C to 25°C and 35°C, respectively. There

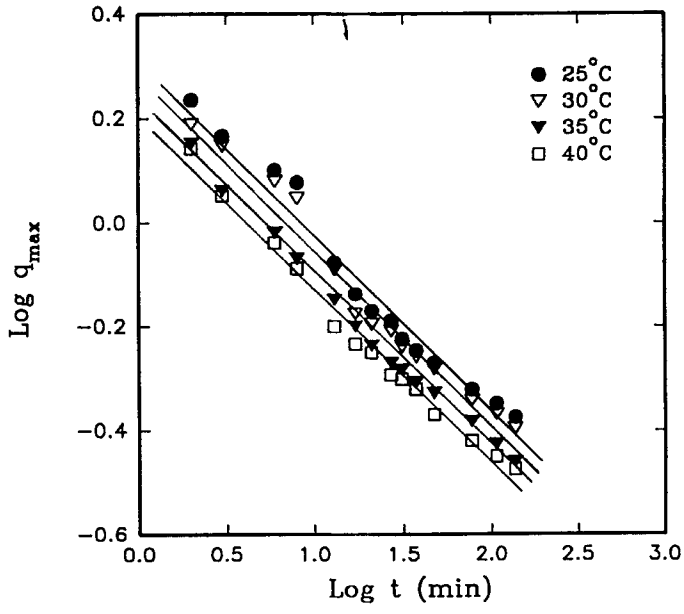

FIGURE 9 Log–log plot of q_{max} vs. t for various deep T quenches (60/40 PS/E7 mixtures).

appears to be no early stage of phase decomposition which can be characterized by the linear Cahn–Hilliard regime.[11] The scattering peak appears in about 1 min and shifts gradually to a smaller wavenumber as time elapses. A cross-over of scattering profiles can be noticed at larger wavenumbers, implying that larger concentration fluctuations (or domains) grow at the expense of smaller fluctuations. Similar results were also obtained for T quenches to 30°C and 40°C.

The shift of wavenumber maxima (q_{max}) and the corresponding peak intensities (I_{max}) with elapsed time is customarily analyzed in terms of power law schemes,[10–15]

$$q_{max} \sim t^{-\alpha} \tag{1}$$

and

$$I_{max} \sim t^{\beta} \tag{2}$$

where α and β are the kinetic exponents which have been predicted by various authors.[12–14] The most common values are $\alpha = 1/3$ and $\beta = 1$ from the evaporation-condensation model by Lifshift and Slyozov[10] and the cluster dynamics model of Binder and Stauffer.[13] Langer, Baron and Miller[14] simulated an exponent $\alpha = 0.21$ by incorporating non-linear terms. On the other hand, Siggia[15] obtained an exponent $\alpha = 1/3$ for the intermediate stage of SD and $\alpha = 1$ at the late stages where the hydrodynamic flow becomes dominant.

Figures 9 and 10 illustrate log–log plots of q_{max} and I_{max} as a function of elapsed time, respectively. For all T quenches, the data can be fit reasonably well by linear slopes with the exponents of $\alpha = 1/3$ and $\beta = 1$, in agreement with the classical evaporation-

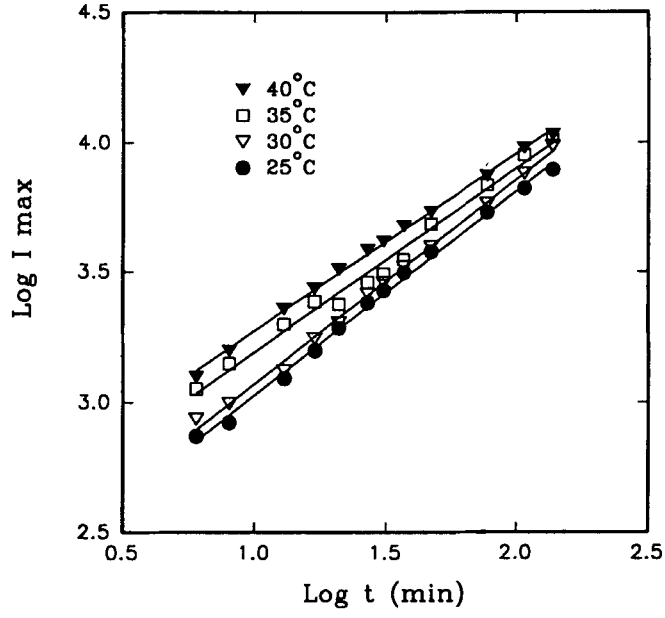

FIGURE 10 Log–log plot of I_{max} vs. t for various deep T quenches (60/40 PS/E7 mixture).

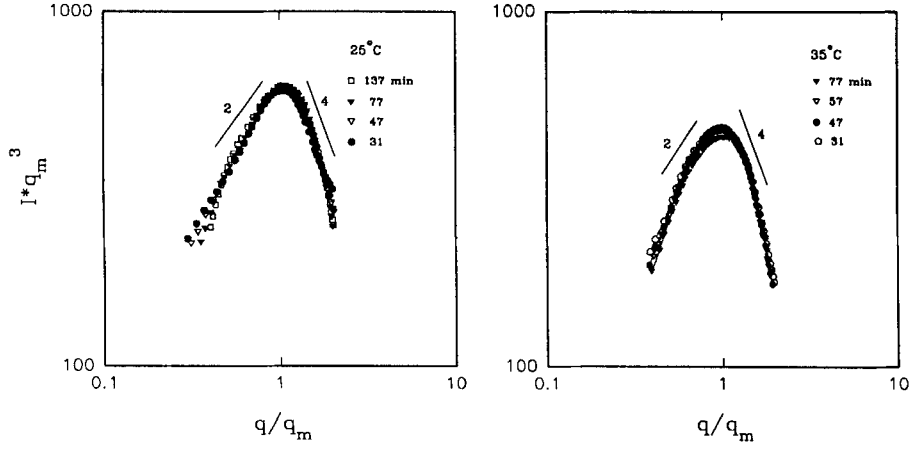

FIGURE 11

condensation theroy[10] and the cluster dynamics model.[13] A similar growth exponent was also experimentally confirmed for various binary systems.[10]

We performed a scaling test for self-similarity in some of the quenches to test whether the structure factor $S(x)$ can be scaled with a single length parameter (ξ) without undergoing any change in geometrical shape of the growing domains;[16] i.e.,

$$I(q,t) \sim V\langle\eta^2\rangle\xi(t)^3 S(x) \tag{3}$$

with

$$x = q\xi(t) \tag{4}$$

where V is the irradiated volume and $\langle \eta^2 \rangle$ the mean square concentration fluctuation. The scaled structure factor can be rewritten as

$$S(x) \sim I(q,t)q_m^3(t) \tag{5}$$

As can be seen in Figure 11, a reasonably good superimposed master curve is obtained when $\log S(x)$ is plotted against $\log q/q_m$, indicating that the system is self-similar and can be scaled with a single length parameter. The slope at $q > q_{max}$ is approximately 4 in conformity with the Furukawa's prediction for an off-critical mixture.[17] According to the Porod law,[18] a slope of 4 is simply the manifestation of sharp and smooth interfaces of the domains. The present results may be not surprising in view of the fact that T quench experiments were deliberately carried out at a composition (60/40 PS/E7) where the effect of orientational order parameter of liquid crystals on dynamics of phase growth is negligibly small. At higher liquid crystal content mixtures, the nematic structure is expected to develop due to the large anisotropy of liquid crystal molecules. Thus, the contribution of orientational order parameter to the free energy could be significant; this will be the subject of a future study.[19]

Acknowledgement

Support of this work by the National Science Foundation through the Science and Technology Center for "Advanced Liquid Crystal Optical Materials: ALCOM" # DMR89-20147 is gratefully acknowledged.

References

1. J. W. Doane, N. A. Vaz, B. G. Wu and S. Zumer, *Appl. Phys. Lett.*, **48**, 269 (1986); J. W. Doane, Liquid Crystals Applications and Uses, B. Bahadur Ed., World Scientific, Ch. 14, 1990.
2. N. A. Vaz, G. W. Smith and G. P. Montgomery, Jr., *Mol. Cryst. Liq. Cryst.*, **146**, 17 (1987).
3. T. Kajiyama, A. Miyamoto, H. Kikuchi and Y. Morimura, *Chem. Lett.*, **1989**, 813 (1989).
4. Y. Hirai, S. Niiyama, H. Kumai and T. Gunjima, SPIE **1257**, 2 (1990); and Rept. Res. Lab. Asahi Glass Co., **40**, 285 (1990).
5. J. L. West, *Mol. Cryst. Liq. Cryst.*, **157**, 427 (1988); and in "Liquid Crystalline Polymers," R. A. Weiss and C. K. Ober, (Eds.) ACS Symp. Series 435, Washington, D.C., Ch. 32, 1990.
6. F. Brochard, J. Jouffroy and P. Levinson, *J. Physique*, **45**, 1125 (1984).
7. P. Palffy-Muhoray, J. J. de Bruyn and D. A. Dunmur, *Mol. Cryst. Liq. Cryst.*, **127**, 301 (1985).
8. T. Kyu, M. Mustafa, J. C. Yang, J. Y. Kim and P. Palffy-Muhoray, in Polymer Solutions, Blends, and Interfaces," I. Noda and D. N. Rubingh, Elsevier, Amsterdam, **245**, 1992.
9. G. W. Smith, *Phys. Rev. Lett.*, **70**, 198 (1993); and *Mol. Cryst. Liq. Cryst.*, **225**, 113 (1993).
10. J. D. Gunton, M. San Miguel and P. S. Sahni, in "Phase Transitions and Critical Phenomenon," C. Domb and J. L. Lebowitz (Eds.) Academic, New York, vol. 8, 1983.
11. A. Cumming, P. Wiltzius and F. S. Bates, *Phys. Rev. Lett.*, **65**, 863 (1990).
12. J. W. Cahn and J. E. Hilliard, *J. Chem. Phys.*, **28**, 258 (1958); J. W. Cahn, *J. Chem. Phys.*, **30**, 1121 (1959).
13. K. Binder and D. Stauffer, *Phys. Rev. Lett.*, **33**, 1006 (1974).
14. J. S. Langer, M. Baron and D. Miller, *Phys. Rev.*, A, **11**, 1417 (1975).
15. E. Siggia, *Phys. Rev.*, 20 A, 595 (1979).
16. H. Furukawa, *Physica* 123 A, 497 (1984).
17. H. Furukawa, *Phys. Rev. B, Rapid Commum.*, **33**, 638 (1986).
18. G. Porod, Kolloid Z., **124**, 83 (1951).
19. C. S. Shen, I. Ilies and T. Kyu, in preparation.